

1 Sensitive response of atmospheric oxidative capacity to the uncertainty in
2 the emissions of nitric oxide (NO) from soils in Amazonia

3
4 Ben H. Lee¹, J. William Munger², Steven C. Wofsy², Luciana V. Rizzo³, James Y. S. Yoon¹,
5 Alexander J. Turner¹, Joel A. Thornton¹, Abigail L. S. Swann¹

6
7 ¹ University of Washington, Seattle, WA, USA

8 ² Harvard University, Cambridge, MA, USA

9 ³ University of São Paulo, São Paulo, SP, Brazil

10
11 Corresponding author: Abigail L. S. Swann (aswann@uw.edu)

12 **Key Points:**

- 13 Soil emission rates of NO in common inventories may be between 10x and 20x too low
14 over the Amazon basin
- 15 Higher soil NO over the Amazon basin alters the oxidative capacity of the atmosphere
16 and decreases global methane lifetime by 1.4% to 2.6%
- 17 Global methane lifetime is more sensitive to Amazon soil NO fluxes than to the loss of
18 terpene fluxes from total deforestation of the Amazon

20 **Abstract**

21 Soils are a major source of nitrogen oxides, which in the atmosphere help govern its oxidative
22 capacity. Thus the response of soil nitric oxide (NO) emissions to forcings such as warming or
23 forest loss has a meaningful impact on global atmospheric chemistry. We find that the soil
24 emission rate of NO in Amazonia from a common inventory is biased low by at least an order of
25 magnitude in comparison to tower-based observations. Accounting for this regional bias
26 decreases the modeled global methane lifetime by 1.4% to 2.6%. In comparison, a fully
27 deforested Amazonia, representing a 37% decrease in global emissions of isoprene, decreases
28 methane lifetime by at most 4.6%, highlighting the sensitive response of oxidation rates to
29 changes in emissions of NO compared to those of terpenes. Our results demonstrate that
30 improving our understanding of soil NO emissions will yield a more accurate representation of
31 atmospheric oxidative capacity.

32

33 **Plain Language Summary**

34 Soils emit a gas called nitric oxide (NO). The amount of NO is emitted from soils in tropical
35 forests is not well known, but has been assumed to be small. We simulated how different
36 amounts of NO emissions from soils in the Amazon impacted atmospheric chemistry. By
37 comparing our modeled results to observations we found that NO emissions from soils in the
38 Amazon may be between 10 and 20 times larger than the current default assumption. This
39 matters because NO reacts in the atmosphere with the gas that is the main gas that reacts with
40 things like methane. Therefore soil NO emissions end up impacting how long methane can last
41 in the atmosphere, and that would have additional climate impacts. Even though soil NO
42 emissions are smaller than other sources of NO emissions globally, we find that the amount of
43 NO emitted in the Amazon matters a lot for how long methane can last in the atmosphere. Our
44 results demonstrate that improving estimates of soil NO emissions is going to be necessary for
45 making accurate estimates of how long methane and other reactive species will stay in the
46 atmosphere.

47

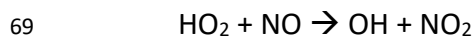
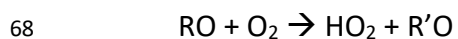
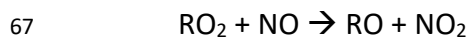
48 **1 Introduction**

49 Nitrogen oxide radicals ($\text{NO}_x = \text{NO} + \text{NO}_2$) play a critical role in regulating the atmosphere's
50 oxidizing capacity through reactions that recycle hydrogen oxides ($\text{HO}_x = \text{OH} + \text{HO}_2$) during the
51 oxidation of hydrocarbons. Accurate representation of this chemistry is crucial, particularly in
52 remote forested regions characterized by relatively low NO_x burdens and high emission rates of
53 biogenic terpenes that give rise to steeply non-linear effects on HO_x , which govern the lifetimes
54 of virtually all hydrocarbons including isoprene and methane. Notably and most recently, *Wells*
55 *et al.* (2020) attributed the high-bias in modeled isoprene levels over Amazonia compared to
56 those observed by the Cross-track Infrared Sounder (CrIS) to a low-bias in NO, likely from soils,
57 causing a low-bias in OH, thus, a runaway increase in modeled isoprene lifetime.

58

59 The atmosphere in and above forests has long been thought to be depressed of hydroxyl (OH)
60 radicals (Jacob & Wofsy, 1988; Logan et al., 1981; Spivakovsky et al., 2000) due to the high
61 concentrations of volatile organic compounds (VOC), which react with OH to form organic
62 peroxy radicals (RO_2), and limited availability of NO_x . In the absence of NO_x , RO_2 will self-react
63 and react with hydro-peroxy radicals (HO_2) to net remove OH and thus depress oxidative
64 capacity. The availability of NO enables the catalytic recycling of OH during the daytime via
65 reactions with RO_2 and HO_2 .

66



71

72 While there have been additional insights into OH recycling pathways from RO_2 chemistry
73 which do not require NO_x , these recycling pathways are not sufficient to explain the Amazon
74 regional observations of isoprene and formaldehyde from satellites (Wells et al., 2020). Tropical
75 forests, and the associated large emissions of reactive VOC, are therefore significant influences
76 on hemispheric if not global oxidizing capacity with consequences for the lifetimes of other
77 trace gases such as methane. In-situ observations of OH and HO_2 in forested environments,

78 however, often show that HO_x concentrations are in fact elevated above expectations (Lelieveld
79 et al., 2008; Tan et al., 2001; Whalley et al., 2011). Implementation of updated chemical
80 mechanisms focused on isoprene – globally the most abundantly emitted volatile organic
81 compound (VOC) (Guenther et al., 2006; Messina et al., 2016) – have elevated modeled HO_x
82 levels (Bates & Jacob, 2019; Squire et al., 2015; Taraborrelli et al., 2012), though robust tests to
83 confirm the validity of those updates remain elusive (Archibald et al., 2010). Recently, *Jeong et al.*
84 *al.* (2022) report that measured OH during the GoAmazon campaign in the 2014 wet season
85 near Manaus, Brazil agreed well with those calculated using multiple chemical models,
86 suggesting that the VOC-RO₂-HO_x-NO_x coupled chemistry is well understood. However, NO
87 measurements during that experiment were unavailable, which is emblematic of the inherent
88 challenges of deployments to such regions where testing of our understanding of emissions and
89 chemistry is most lacking.

90
91 The sensitivity of the burden and lifetime of methane to global OH levels is well studied (Squire
92 et al., 2015; Voulgarakis et al., 2013; Wild et al., 2020; Zhao et al., 2020). The role that
93 anthropogenic NO_x plays in governing OH and therefore methane levels is also well
94 documented (Laughner et al., 2021; Peng et al., 2022; Stevenson et al., 2022). Less emphasis
95 has been placed on the role of NO_x from natural sources, though *Song et al.* (2021) report that
96 approximately half of atmospheric NO_x is now derived from sources other than fossil fuel
97 combustion. Soils produce NO through nitrification/denitrification with subsequent emission to
98 the atmosphere moderated by a suite of environmental conditions including soil type, gas
99 diffusivity, moisture, temperature, etc. Alterations to forests, whether through conversion to
100 pasture or logging, will consequently result in changes to soil emissions (Garcia-Montiel et al.,
101 2001; Keller et al., 2005).

102
103 Numerous global chemical models – including the Community Atmosphere Model (CESM2-
104 CAM-Chem) utilized here – refer to the work of *Yienger and Levy* (1995) to constrain soil NO
105 emissions. More recent work by *Hudman et al.* (2012), on which *Wells et al.* (2020) rely,
106 developed an updated parameterization including a more physical representation of soil

107 processes derived from field observations that yielded greater soil NO emissions globally (10.7
108 Tg N yr⁻¹) compared to that of Yienger and Levy (7.4 Tg N yr⁻¹), though rates over Amazonia are
109 significantly lower due likely to the inclusion of NO_x loss on canopy surfaces. Discrepancies
110 amongst published inventories additionally highlight the uncertainty in soil emission rates of
111 NO (Davidson, 1993; Ganzeveld et al., 2002; Jaeglé et al., 2005; Martin et al., 2003; Yan et al.,
112 2005), the tropospheric abundance of which is not reliably inferred from space.

113

114 We present the sensitivity of the oxidative capacity of the atmosphere, and specifically, the
115 global lifetime of methane as a function of increasing soil NO emission rates over just the
116 Amazon region as supported by in-situ observations at the Tapajos National Forest (54.580°W,
117 2.51°S, Pará, Brazil) from January to August of 2015. We compare this scenario to a set of
118 simulations in which the region is fully deforested leading to a near ceasing of the emissions of
119 biogenic terpenes, which are known to have implications on chemistry and climate (L.
120 Ganzeveld et al., 2010; L. Ganzeveld & Lelieveld, 2004; Geddes et al., 2016; Heald & Spracklen,
121 2015; Keller et al., 2005; Lathière et al., 2006; Opacka et al., 2021; Unger, 2014; Wiedinmyer et
122 al., 2006; Wu et al., 2012). Results presented here demonstrate the importance of capturing
123 not only the magnitude of NO emissions but responses to evolving conditions given the
124 sensitive response of the oxidative capacity, particularly in and above forests in tropical regions
125 where methane oxidation is likely fastest and least certain (Turner et al., 2019).

126

127 **2 Methods**

128 We performed six sets of coupled biosphere-atmospheric chemistry simulations using the
129 CESM2-CAM-Chem global model (Danabasoglu et al., 2020; Emmons et al., 2010) with active
130 biogeochemistry at ~1° spatial resolution. Three separate sets were initialized with forests in
131 Amazonia in a state that is representative of the early 1980s. The other three were initialized
132 with Amazonia that was effectively devoid of trees by changing the plant functional type to a
133 grassland over the region (from 16°S to 8°N and from 48°W to 78°W), as illustrated in **Figure S1**.
134 Leaf area is calculated prognostically, as are other carbon fluxes and pools, however,
135 atmospheric CO₂ concentrations are specified based on observed concentrations for each year.

136 The removal of trees in the model changes physical fluxes of energy and water, as well as carbon
137 and chemical species (e.g. isoprene). The model calculated total leaf area index is about 6.5 m^2
138 m^{-2} in the forested scenarios and about $1.8 \text{ m}^2 \text{ m}^{-2}$ in the deforested scenario, wherein the
139 emission rates of biogenic terpenes including isoprene and monoterpenes are negligible. For
140 each of the forested and deforested Amazonia scenarios we calculated three sets of simulations
141 representing different soil NO conditions: (i) baseline soil NO emission rate based on the work
142 of *Yienger and Levy (1995)*, and factors of (ii) $10\times$ that rate, and (ii) $20\times$ of that rate. All
143 simulation scenarios span from 2001 to 2005, except for the forested baseline soil NO scenario
144 which spans from 1980 to 2015. All aspects of the model except for plant type and soil NO
145 fluxes within the Amazon vary transiently across years based on observed quantities, including
146 greenhouse gas concentrations, sea surface temperatures, and land cover change outside the
147 Amazon basin (“FCfireHIST” compset in CESM2).

148
149 We also utilized FOAM (Framework for 0-D Atmospheric Modeling; Wolfe et al., 2016), which
150 leverages the more comprehensive Master Chemical Mechanism (MCM) version 3.3.1 (Jenkin et
151 al., 2015; Jenkin et al., 1997; Saunders et al., 2003) to compare against the CESM2-CAM-Chem
152 results. We performed a series of simulations. Each was conducted with constant introduction
153 rates of NO, O₃, and isoprene into the well-mixed volume with active photochemistry ($J_{\text{NO}_2} =$
154 $2\times 10^{-2} \text{ s}^{-1}$), and allowed to evolve for 60 hours, much longer than the time needed for all species
155 to reach steady state. The rate of NO introduction was varied widely to capture the response of
156 oxidation chemistry to the steady state NO mixing ratios, while the rates of introduction of O₃
157 and isoprene were set such that the steady state resulting mixing ratios were comparable to the
158 levels reported by CESM2-CAM-Chem for the three soil NO emission rate scenarios. We
159 compare in the section below the levels OH and HO₂ calculated by CESM2-CAM-Chem and
160 FOAM.

161
162 Mixing ratios of NO, nitrogen dioxide (NO₂), and O₃ were measured at the Tapajos National
163 Forest from January to August of 2015. Ambient air in excess of instrument requirements was
164 drawn in at 4-6 liters per minute (lpm) through inlets located at eight heights off of the tall

165 tower (0.91, 3.05, 10.42, 19.57, 28.71, 39.41, 53.04, 62.24 m above the ground). The NO
166 chemiluminescence analyzer drew ~2 lpm and the O₃ analyzer drew ~1 lpm. Excess flow was
167 pulled by a bypass pump to maintain constant pressure measured by a pressure controller. The
168 inlets were sampled in sequence for 4 minutes each. NO and NO₂ were measured by an
169 EcoPhysics CLD-780TR analyzer equipped with an external NO₂ photolysis cell using a
170 Hamamatsu LED with peak wavelength at 365 nm (Pollack et al., 2010). The photolysis cell was
171 toggled on and off at 60 s intervals to provide both NO and NO + NO₂ measurement at each
172 sample height. All instruments were housed in an air conditioned shed near the base of the
173 tower. Instrument background signal was measured by periodically adding O₃ generated by a
174 Hg-vapor lamp to the sample stream to convert NO to NO₂ before the sample entered the
175 detector. Instrument gain and NO₂ conversion efficiency were determined by routinely adding a
176 small flow of NO or NO₂ standard to the sample inlet.

177

178 **3 Results and Discussion**

179 In comparison to the measurements made above the forest canopy, CESM2-CAM-Chem
180 underestimates NO mixing ratio in the lower-most level of the atmosphere in the model-grid
181 encompassing the Tapajos National Forest, when utilizing the baseline soil NO emission rate as
182 prescribed by the work of Yienger and Levy (1995) (**Figures 1a and S2**). Observed vertical profile
183 from 0.9 m to 62 m from the forest floor show that NO is most abundant near the forest floor,
184 elevated to as high as a few parts per billion (ppb). Its mixing ratio decreases with height
185 predominantly as it reacts with O₃ to form NO₂ (Bakwin et al., 1990), indicating that the
186 dominant NO source at this site is likely from the soil underneath the forest canopy, and
187 negligibly from an upwind source. The years 2015 and 2016 were characterized by El Niño
188 conditions. The resulting drier-than-normal conditions in Amazonia could have contributed to
189 higher than normal soil NO emissions, which exhibit a non-linear response to changing soil
190 moisture levels (Davidson, 1993; Davidson & Kinglerlee, 1997; Garcia-Montiel et al., 2001; Gut et
191 al., 2002; Luo et al., 2012). However, El Niño became active at earliest in March of 2015,
192 whereas the model underestimates observations throughout the year with no noticeable
193 change in the model-observation discrepancy around that time. Biomass burning as well does

194 not appear to have had a significant long-term impact on NO levels at the site given that the
195 observations at the top of the tower do not exhibit periodic bursts or enhancements associated
196 with influence from fresh or intense combustion sources (**Figure S2**).

197
198 Observed NO₂ and O₃ levels are, likewise, greater than those modeled for the lowest level of the
199 atmosphere when implementing the baseline soil NO emission rate. One implication is that the
200 modeled oxidative capacity of the atmosphere, namely OH and HO₂, is also likely biased low
201 given NO cycles HO₂ to OH and that O₃ is the dominant primary HO_x source. As such, increasing
202 the model soil NO emission rate enhances the levels of NO_x, HO_x and O₃, as shown in **Figure 1**
203 **(and Figures S3, S4, and S5)**. The median level of NO measured above the forest canopy
204 generally resides between that modeled with 10× and 20× soil emission rates. Similarly,
205 modeled soil NO emission rates at 10x and 20x also show closer agreement with measured soil
206 NO emission rates from unperturbed tropical forests (**Figure S7**). The mean ratios of the
207 observed to modeled NO_x resulting from utilizing the baseline, 10×, and 20× soil emission rates
208 are 2.7, 0.7, and 0.4, respectively.

209
210 With the enhanced soil emission rates, OH – though never measured at the Tapajos National
211 Forest – increases to levels that are well within an order of magnitude of that observed during
212 the GoAmazon experiment (Jeong et al., 2022) (**Figure 2d**), with corresponding effects on the
213 lifetime and burden of isoprene. However, the modeled isoprene mixing ratio still overestimates
214 observations at the Tapajos National Forest made in June of 2016 (Sarkar et al., 2020) by a
215 factor between 8 and 12 (**Figure 2c**). This discrepancy is not due to inaccurate isoprene fluxes
216 (**Figure 2b**), which at the site agrees well between what is measured by the eddy covariance
217 approach and modeled using MEGAN (Model of Emissions of Gases and Aerosols from Nature; ,
218 which also constrains biogenic terpene emissions for CESM2-CAM-Chem.

219
220 In addition to a low bias in soil NO emission rate, mixing in the boundary layer within CESM2-
221 CAM-Chem is likely too slow. The vertical profile of modeled NO in the boundary layer exhibits a
222 sharp enhancement in the lowest level of the atmosphere that interacts with the surface where

223 emissions are continuously occurring (**Figure S3**) with O₃ showing a corresponding depletion
224 (**Figure S4**), comparable to what is observed from the tower beneath the forest canopy (**Figure**
225 **1**). Such erroneously slow vertical mixing leads to excessive accumulation of NO in the lower-
226 most layer of the atmosphere and deprives the rest of the boundary layer of NO (and isoprene)
227 that would otherwise lead to enhanced O₃ and HO_x levels, and therefore a shorter isoprene
228 lifetime. Faster boundary layer mixing in the model would lead to dilution of NO in the surface
229 layer and would in turn require an even stronger surface NO flux than what we have
230 implemented here in order to match what was observed at the Tapajos National Forest. As such,
231 the soil NO emission rate we infer here is likely a lower bound on the truth due to the slow
232 mixing in CESM2-CAM-Chem.

233
234 There is good agreement between OH and HO₂ concentrations determined for the three forested
235 simulations of varying soil NO emission rates and those of the F0AM simulations (**Figure S8**)
236 indicating that all significant chemical mechanisms listed in the more comprehensive MCM v3.3.1
237 (Jenkin et al., 2015; Jenkin et al., 1997; Saunders et al., 2003) are represented by the chemistry
238 module of CESM2-CAM-Chem which is more condensed. Therefore, the high-bias in isoprene
239 mixing ratios (**Figure 2c**) is likely not the result of deficient chemistry in CESM2-CAM-Chem.

240
241 We also note the variability in the observed NO values, as evidenced by the large difference in
242 the observed mean and observed median NO mixing ratios (**Figure 2**). This is likely due to the
243 dependence of nitrification and denitrification that generate NO on changes to conditions such
244 as soil humidity and soil temperature. The modeled NO levels are much less variable – denoted
245 by the shaded trace for a given month that represent the variability between the years 2001
246 and 2005 – since its emissions are based on seasonally-varying but annually-repeating
247 climatology. The minimum and maximum soil NO flux in the model region corresponding to the
248 Tapajos National Forest are 2.0×10^9 and 2.8×10^9 molecules cm⁻² s⁻¹, respectively. As a result, the
249 response of soil NO emissions to varying environmental conditions is not readily captured
250 currently by CESM2-CAM-Chem.

251

252 The resulting increase in OH due to increasing the soil NO emission rate of Amazonia is
253 significant enough to be globally relevant. We find that there is about a 3-fold increase in the
254 fractional change in OH number concentration below 800 hPa in response to increasing the
255 baseline soil emission rate by a factor of 20× (**Figure 3**). The factors of 10× and 20× increases in
256 soil NO emission rates relative to baseline rates lead to 2.6% and 5.5% increases in the total
257 (natural and anthropogenic) global surface NO_x emissions (**Figure 4b**), and cause decreases in
258 the global methane lifetime of 1.4% and 2.6%, respectively (**Figure 4a**). For context, this is
259 approaching the amount needed to resolve the stabilization of methane observed between the
260 years 2000 and 2007 (Dlugokencky et al., 2003; Lan et al., 2022), which can be explained by an
261 approximately 4% increase in global OH levels as supported by remote-site measurements of
262 methyl chloroform (Rigby et al., 2017; Turner et al., 2017), and which remains yet unresolved
263 by models (Stevenson et al., 2020; Turner et al., 2019).

264
265 We compare the global methane lifetime's sensitivity to changes in Amazonian soil NO_x
266 emissions and terpene emissions. Nearly ceasing Amazonia's emissions of biogenic terpenes
267 including isoprene through simulated deforestation causes a 37% decrease in the global
268 isoprene emission rate (**Figure 4c**) but only a 4.6% decrease in the global methane lifetime. That
269 a much larger change in isoprene emissions compared to NO emissions is required to induce a
270 comparable change in OH illustrates the much higher sensitivity of global OH levels and
271 methane lifetime to the emission rate of NO relative to that of terpenes. Lastly, simulating
272 deforestation with a dynamic biosphere model shows its impact on soil characteristics such as
273 moisture and soil temperature (**Figure S9**), both of which drive nitrification and denitrification
274 processes that generate NO (Davidson et al., 2000; Garcia-Montiel et al., 2001; Luo et al., 2012),
275 alongside a suite of other variables such as soil and tree types, extents of nitrogen input, and
276 history of land-use (Bakwin et al., 1990; Erickson et al., 2002; Koehler et al., 2009; Pilegaard et
277 al., 2006). These results call for the need for a dynamic soil model for NO emissions capable of
278 incorporating the response of soil nitrogen processing to changes in environmental conditions,
279 to adequately represent and forecast atmospheric oxidative chemistry.

280

281 **4 Conclusions**

282 Emission rates of NO from soils in CESM2-CAM-Chem are underestimated by at least an order
283 of magnitude compared to ground-based observations of NO_x fluxes, partitioning and vertical
284 profiles. Factors that likely contribute to the low-bias in existing inventories include inadequate
285 number of field measurements encompassing multiple seasons in numerous land types that
286 provide model constraints, as well as implementation of overly aggressive NO_x loss on forest
287 canopy surfaces. We show that correcting this low-bias in NO_x emissions enhances regional OH
288 levels to such an extent as to be globally significant. The soil NO emission rate over Amazonia
289 was increased by a factor of 10× to 20× relative to the rates prescribed by Yienger and Levy
290 (Yienger & Levy II, 1995) to achieve consistency with observations at the Tapajos National
291 Forest, resulting in a global average methane lifetime decreases of 1.4% and 2.6%, respectively.
292 The extent of NO flux underestimation may be even greater if the model utilized here suffers
293 from slow vertical mixing of the boundary layer. The impact on the global oxidative capacity
294 due to such increases in soil NO emissions over Amazonia is comparable to that due to the near
295 complete ceasing of biogenic VOC emissions from the deforestation of Amazonia. Given the
296 sensitivity of the global atmospheric oxidative capacity to relatively small changes in our
297 current estimation of global NO_x emissions, understanding the magnitude and sign of the
298 response of soil NO emissions to past and future forcings including land use and land cover
299 change are critical for assessing the lifetimes of all reactive species of the atmosphere.

300

301 **Acknowledgements**

302 ALSS and BHL acknowledge NSF Macrosystems award to the University of Washington DEB-
303 1925837. LVR acknowledges the Sao Paulo State Funding Agency (FAPESP 10156-8/2013).
304 JAT acknowledges an award from the NSF Atmospheric and Geo-space Sciences AGS-2023670.
305 Trace gas observations at the Tapajos km67 site were supported by Department of Energy
306 Grant # DE-SC0008311. We especially thank the staff at the LBA office in Santarem for logistical
307 support.

308

309 **Open Research**

310 The observations made at the Tapajos National Forest as well as the model simulation output
311 described in this paper are available through Dryad (available at this link during peer review:
312 <https://datadryad.org/stash/share/uWEs8q4jBPor-wijYBwdnmacFixCaNWV10yXIGxQzlo>, final
313 DOI to be provided after manuscript is accepted).

314

315 **References**

316 Archibald, A. T., Cooke, M. C., Utembe, S. R., Shallcross, D. E., Derwent, R. G., & Jenkin, M. E.
317 (2010). Impacts of mechanistic changes on HO_x formation and recycling in the oxidation of
318 isoprene. *Atmospheric Chemistry and Physics*, *10*(17), 8097–8118.
319 <https://doi.org/10.5194/acp-10-8097-2010>

320 Bakwin, P. S., Wofsy, S. C., Fan, S.-M., Keller, M., Trumbore, S. E., & Da Costa, J. M. (1990).
321 Emission of nitric oxide (NO) from tropical forest soils and exchange of NO between the
322 forest canopy and atmospheric boundary layers. *Journal of Geophysical Research:*
323 *Atmospheres*, *95*(D10), 16755–16764. <https://doi.org/10.1029/JD095iD10p16755>

324 Bates, K. H., & Jacob, D. J. (2019). A new model mechanism for atmospheric oxidation of
325 isoprene: global effects on oxidants, nitrogen oxides, organic products, and secondary
326 organic aerosol. *Atmospheric Chemistry and Physics*, *19*(14), 9613–9640.
327 <https://doi.org/10.5194/acp-19-9613-2019>

328 Danabasoglu, G., Lamarque, J.-F., Bacmeister, J., Bailey, D. A., DuVivier, A. K., Edwards, J., et al.
329 (2020). The Community Earth System Model Version 2 (CESM2). *Journal of Advances in*
330 *Modeling Earth Systems*, *12*(2), e2019MS001916. <https://doi.org/10.1029/2019MS001916>

331 Davidson, E. A. (1993). Soil Water Content and the Ratio of Nitrous Oxide to Nitric Oxide Emitted
332 from Soil. In R. S. Oremland (Ed.), *Biogeochemistry of Global Change: Radiatively Active*
333 *Trace Gases Selected Papers from the Tenth International Symposium on Environmental*
334 *Biogeochemistry, San Francisco, August 19–24, 1991* (pp. 369–386). Boston, MA: Springer
335 US. https://doi.org/10.1007/978-1-4615-2812-8_20

336 Davidson, E. A., & Kingerlee, W. (1997). A global inventory of nitric oxide emissions from soils.
337 *Nutrient Cycling in Agroecosystems*, *48*(1), 37–50.
338 <https://doi.org/10.1023/A:1009738715891>

339 Davidson, E. A., Keller, M., Erickson, H. E., Verchot, L. V., & Veldkamp, E. (2000). Testing a
340 Conceptual Model of Soil Emissions of Nitrous and Nitric Oxides: Using two functions based
341 on soil nitrogen availability and soil water content, the hole-in-the-pipe model characterizes
342 a large fraction of the observed variation of nitric oxide and nitrous oxide emissions from
343 soils. *BioScience*, *50*(8), 667–680. [https://doi.org/10.1641/0006-](https://doi.org/10.1641/0006-3568(2000)050[0667:TACMOS]2.0.CO;2)
344 [3568\(2000\)050\[0667:TACMOS\]2.0.CO;2](https://doi.org/10.1641/0006-3568(2000)050[0667:TACMOS]2.0.CO;2)

345 Dlugokencky, E. J., Houweling, S., Bruhwiler, L., Masarie, K. A., Lang, P. M., Miller, J. B., & Tans, P.
346 P. (2003). Atmospheric methane levels off: Temporary pause or a new steady-state?
347 *Geophysical Research Letters*, *30*(19). <https://doi.org/10.1029/2003GL018126>

348 Emmons, L. K., Walters, S., Hess, P. G., Lamarque, J.-F., Pfister, G. G., Fillmore, D., et al. (2010).
349 Description and evaluation of the Model for Ozone and Related chemical Tracers, version 4
350 (MOZART-4). *Geoscientific Model Development*, *3*(1), 43–67. [https://doi.org/10.5194/gmd-3-](https://doi.org/10.5194/gmd-3-43-2010)
351 [43-2010](https://doi.org/10.5194/gmd-3-43-2010)

352 Erickson, H., Davidson, E. A., & Keller, M. (2002). Former land-use and tree species affect
353 nitrogen oxide emissions from a tropical dry forest. *Oecologia*, *130*(2), 297–308.
354 <https://doi.org/10.1007/s004420100801>

355 Ganzeveld, L., & Lelieveld, J. (2004). Impact of Amazonian deforestation on atmospheric
356 chemistry. *Geophysical Research Letters*, *31*(6). <https://doi.org/10.1029/2003GL019205>

357 Ganzeveld, L., Bouwman, L., Stehfest, E., van Vuuren, D. P., Eickhout, B., & Lelieveld, J. (2010).
358 Impact of future land use and land cover changes on atmospheric chemistry-climate
359 interactions. *Journal of Geophysical Research: Atmospheres*, *115*(D23).
360 <https://doi.org/10.1029/2010JD014041>

361 Ganzeveld, L. N., Lelieveld, J., Dentener, F. J., Krol, M. C., Bouwman, A. J., & Roelofs, G.-J. (2002).
362 Global soil-biogenic NO_x emissions and the role of canopy processes. *Journal of Geophysical*
363 *Research: Atmospheres*, *107*(D16), ACH 9-1-ACH 9-17.
364 <https://doi.org/10.1029/2001JD001289>

365 Garcia-Montiel, D. C., Steudler, P. A., Piccolo, M. C., Melillo, J. M., Neill, C., & Cerri, C. C. (2001).
366 Controls on soil nitrogen oxide emissions from forest and pastures in the Brazilian Amazon.
367 *Global Biogeochemical Cycles*, *15*(4), 1021–1030. <https://doi.org/10.1029/2000GB001349>

368 Geddes, J. A., Heald, C. L., Silva, S. J., & Martin, R. V. (2016). Land cover change impacts on
369 atmospheric chemistry: simulating projected large-scale tree mortality in the United States.
370 *Atmospheric Chemistry and Physics*, 16(4), 2323–2340. [https://doi.org/10.5194/acp-16-](https://doi.org/10.5194/acp-16-2323-2016)
371 2323-2016

372 Guenther, A., Karl, T., Harley, P., Wiedinmyer, C., Palmer, P. I., & Geron, C. (2006). Estimates of
373 global terrestrial isoprene emissions using MEGAN (Model of Emissions of Gases and
374 Aerosols from Nature). *Atmospheric Chemistry and Physics*, 6(11), 3181–3210.
375 <https://doi.org/10.5194/acp-6-3181-2006>

376 Gut, A., van Dijk, S. M., Scheibe, M., Rummel, U., Welling, M., Ammann, C., et al. (2002). NO
377 emission from an Amazonian rain forest soil: Continuous measurements of NO flux and soil
378 concentration. *Journal of Geophysical Research: Atmospheres*, 107(D20), LBA 24-1-LBA 24-
379 10. <https://doi.org/10.1029/2001JD000521>

380 Heald, C. L., & Spracklen, D. V. (2015). Land Use Change Impacts on Air Quality and Climate.
381 *Chemical Reviews*, 115(10), 4476–4496. <https://doi.org/10.1021/cr500446g>

382 Hudman, R. C., Moore, N. E., Mebust, A. K., Martin, R. V., Russell, A. R., Valin, L. C., & Cohen, R.
383 C. (2012). Steps towards a mechanistic model of global soil nitric oxide emissions:
384 implementation and space based-constraints. *Atmospheric Chemistry and Physics*, 12(16),
385 7779–7795. <https://doi.org/10.5194/acp-12-7779-2012>

386 Jacob, D. J., & Wofsy, S. C. (1988). Photochemistry of biogenic emissions over the Amazon
387 forest. *Journal of Geophysical Research: Atmospheres*, 93(D2), 1477–1486.
388 <https://doi.org/10.1029/JD093iD02p01477>

389 Jaeglé, L., Steinberger, L., Martin, R.V., and Chance, K. (2005). Global partitioning of NO_x sources
390 using satellite observations: Relative roles of fossil fuel combustion , biomass burning and
391 soil emissions. *Faraday Discussions*, 130(0):407–423. <https://doi.org/10.1039/B502128F>

392 Jenkin, M. E., Young, J. C., & Rickard, A. R. (2015). The MCM v3.3.1 degradation scheme for
393 isoprene. *Atmospheric Chemistry and Physics*, 15(20), 11433–11459.
394 <https://doi.org/10.5194/acp-15-11433-2015>

395 Jenkin, Michael E., Saunders, S. M., & Pilling, M. J. (1997). The tropospheric degradation of
396 volatile organic compounds: a protocol for mechanism development. *Atmospheric*
397 *Environment*, 31(1), 81–104. [https://doi.org/10.1016/S1352-2310\(96\)00105-7](https://doi.org/10.1016/S1352-2310(96)00105-7)

398 Jeong, D., Seco, R., Emmons, L., Schwantes, R., Liu, Y., McKinney, K. A., et al. (2022). Reconciling
399 Observed and Predicted Tropical Rainforest OH Concentrations. *Journal of Geophysical*
400 *Research: Atmospheres*, 127(1), e2020JD032901. <https://doi.org/10.1029/2020JD032901>

401 Keller, M., Varner, R., Dias, J. D., Silva, H., Crill, P., Oliveira, R. C. de, & Asner, G. P. (2005). Soil–
402 Atmosphere Exchange of Nitrous Oxide, Nitric Oxide, Methane, and Carbon Dioxide in
403 Logged and Undisturbed Forest in the Tapajos National Forest, Brazil. *Earth Interactions*,
404 9(23), 1–28. <https://doi.org/10.1175/EI125.1>

405 Koehler, B., Corre, M. D., Veldkamp, E., Wullaert, H., & Wright, S. J. (2009). Immediate and long-
406 term nitrogen oxide emissions from tropical forest soils exposed to elevated nitrogen input.
407 *Global Change Biology*, 15(8), 2049–2066. [https://doi.org/10.1111/j.1365-](https://doi.org/10.1111/j.1365-2486.2008.01826.x)
408 2486.2008.01826.x

409 Lan, X., Thoning, K. W., & Dlugokenchy, E. J. (2022). Trends in globally-averaged CH₄, N₂O, and
410 SF₆ determined from NOAA Global Monitoring Laboratory measurements (Version Version
411 2023-09) [Data set]. Retrieved from <https://doi.org/10.15138/P8XG-AA10>

412 Lathière, J., Hauglustaine, D. A., Friend, A. D., De Noblet-Ducoudré, N., Viovy, N., & Folberth, G.
413 A. (2006). Impact of climate variability and land use changes on global biogenic volatile
414 organic compound emissions. *Atmospheric Chemistry and Physics*, 6(8), 2129–2146.
415 <https://doi.org/10.5194/acp-6-2129-2006>

416 Laughner, J. L., Neu, J. L., Schimel, D., Wennberg, P. O., Barsanti, K., Bowman, K. W., et al. (2021).
417 Societal shifts due to COVID-19 reveal large-scale complexities and feedbacks between
418 atmospheric chemistry and climate change. *Proceedings of the National Academy of*
419 *Sciences*, 118(46), e2109481118. <https://doi.org/10.1073/pnas.2109481118>

420 Lelieveld, J., Butler, T. M., Crowley, J. N., Dillon, T. J., Fischer, H., Ganzeveld, L., et al. (2008).
421 Atmospheric oxidation capacity sustained by a tropical forest. *Nature*, 452(7188), 737–740.
422 <https://doi.org/10.1038/nature06870>

423 Logan, J. A., Prather, M. J., Wofsy, S. C., & McElroy, M. B. (1981). Tropospheric chemistry: A
424 global perspective. *Journal of Geophysical Research: Oceans*, *86*(C8), 7210–7254.
425 <https://doi.org/10.1029/JC086iC08p07210>

426 Luo, G. J., Brüggemann, N., Wolf, B., Gasche, R., Grote, R., & Butterbach-Bahl, K. (2012). Decadal
427 variability of soil CO₂, NO, N₂O, and CH₄ fluxes at the Höglwald Forest, Germany.
428 *Biogeosciences*, *9*(5), 1741–1763. <https://doi.org/10.5194/bg-9-1741-2012>

429 Martin, R. V., Jacob, D. J., Chance, K., Kurosu, T. P., Palmer, P. I., & Evans, M. J. (2003). Global
430 inventory of nitrogen oxide emissions constrained by space-based observations of NO₂
431 columns. *Journal of Geophysical Research: Atmospheres*, *108*(D17).
432 <https://doi.org/10.1029/2003JD003453>

433 Messina, P., Lathière, J., Sindelarova, K., Vuichard, N., Granier, C., Ghattas, J., et al. (2016). Global
434 biogenic volatile organic compound emissions in the ORCHIDEE and MEGAN models and
435 sensitivity to key parameters. *Atmospheric Chemistry and Physics*, *16*(22), 14169–14202.
436 <https://doi.org/10.5194/acp-16-14169-2016>

437 Opacka, B., Müller, J.-F., Stavrakou, T., Bauwens, M., Sindelarova, K., Markova, J., & Guenther, A.
438 B. (2021). Global and regional impacts of land cover changes on isoprene emissions derived
439 from spaceborne data and the MEGAN model. *Atmospheric Chemistry and Physics*, *21*(11),
440 8413–8436. <https://doi.org/10.5194/acp-21-8413-2021>

441 Peng, S., Lin, X., Thompson, R. L., Xi, Y., Liu, G., Hauglustaine, D., et al. (2022). Wetland emission
442 and atmospheric sink changes explain methane growth in 2020. *Nature*, *612*(7940), 477–
443 482. <https://doi.org/10.1038/s41586-022-05447-w>

444 Pilegaard, K., Skiba, U., Ambus, P., Beier, C., Brüggemann, N., Butterbach-Bahl, K., et al. (2006).
445 Factors controlling regional differences in forest soil emission of nitrogen oxides (NO and
446 N₂O). *Biogeosciences*, *3*(4), 651–661. <https://doi.org/10.5194/bg-3-651-2006>

447 Pollack, I. B., Lerner, B. M., & Ryerson, T. B. (2010). Evaluation of ultraviolet light-emitting diodes
448 for detection of atmospheric NO₂ by photolysis - chemiluminescence. *Journal of*
449 *Atmospheric Chemistry*, *65*(2), 111–125. <https://doi.org/10.1007/s10874-011-9184-3>

450 Rigby, M., Montzka, S. A., Prinn, R. G., White, J. W. C., Young, D., O'Doherty, S., et al. (2017). Role
451 of atmospheric oxidation in recent methane growth. *Proceedings of the National Academy
452 of Sciences*, *114*(21), 5373–5377. <https://doi.org/10.1073/pnas.1616426114>

453 Sarkar, C., Guenther, A. B., Park, J.-H., Seco, R., Alves, E., Batalha, S., et al. (2020). PTR-TOF-MS
454 eddy covariance measurements of isoprene and monoterpene fluxes from an eastern
455 Amazonian rainforest. *Atmospheric Chemistry and Physics*, *20*(12), 7179–7191.
456 <https://doi.org/10.5194/acp-20-7179-2020>

457 Saunders, S. M., Jenkin, M. E., Derwent, R. G., & Pilling, M. J. (2003). Protocol for the
458 development of the Master Chemical Mechanism, MCM v3 (Part A): tropospheric
459 degradation of non-aromatic volatile organic compounds. *Atmospheric Chemistry and
460 Physics*, *3*(1), 161–180. <https://doi.org/10.5194/acp-3-161-2003>

461 Song, W., Liu, X.-Y., Hu, C.-C., Chen, G.-Y., Liu, X.-J., Walters, W. W., et al. (2021). Important
462 contributions of non-fossil fuel nitrogen oxides emissions. *Nature Communications*, *12*(1),
463 243. <https://doi.org/10.1038/s41467-020-20356-0>

464 Spivakovsky, C. M., Logan, J. A., Montzka, S. A., Balkanski, Y. J., Foreman-Fowler, M., Jones, D. B.
465 A., et al. (2000). Three-dimensional climatological distribution of tropospheric OH: Update
466 and evaluation. *Journal of Geophysical Research: Atmospheres*, *105*(D7), 8931–8980.
467 <https://doi.org/10.1029/1999JD901006>

468 Squire, O. J., Archibald, A. T., Griffiths, P. T., Jenkin, M. E., Smith, D., & Pyle, J. A. (2015). Influence
469 of isoprene chemical mechanism on modelled changes in tropospheric ozone due to climate
470 and land use over the 21st century. *Atmospheric Chemistry and Physics*, *15*(9), 5123–5143.
471 <https://doi.org/10.5194/acp-15-5123-2015>

472 Stevenson, D. S., Zhao, A., Naik, V., O'Connor, F. M., Tilmes, S., Zeng, G., et al. (2020). Trends in
473 global tropospheric hydroxyl radical and methane lifetime since 1850 from AerChemMIP.
474 *Atmospheric Chemistry and Physics*, *20*(21), 12905–12920. [https://doi.org/10.5194/acp-20-
475 12905-2020](https://doi.org/10.5194/acp-20-12905-2020)

476 Stevenson, D. S., Derwent, R. G., Wild, O., & Collins, W. J. (2022). COVID-19 lockdown emission
477 reductions have the potential to explain over half of the coincident increase in global

478 atmospheric methane. *Atmospheric Chemistry and Physics*, 22(21), 14243–14252.
479 <https://doi.org/10.5194/acp-22-14243-2022>

480 Tan, D., Faloon, I., Simpas, J. B., Brune, W., Shepson, P. B., Couch, T. L., et al. (2001). HO x
481 budgets in a deciduous forest: Results from the PROPHET summer 1998 campaign. *Journal*
482 *of Geophysical Research: Atmospheres*, 106(D20), 24407–24427.
483 <https://doi.org/10.1029/2001JD900016>

484 Taraborrelli, D., Lawrence, M. G., Crowley, J. N., Dillon, T. J., Gromov, S., Groß, C. B. M., et al.
485 (2012). Hydroxyl radical buffered by isoprene oxidation over tropical forests. *Nature*
486 *Geoscience*, 5(3), 190–193. <https://doi.org/10.1038/ngeo1405>

487 Turner, A. J., Frankenberg, C., Wennberg, P. O., & Jacob, D. J. (2017). Ambiguity in the causes for
488 decadal trends in atmospheric methane and hydroxyl. *Proceedings of the National Academy*
489 *of Sciences*, 114(21), 5367–5372. <https://doi.org/10.1073/pnas.1616020114>

490 Turner, A. J., Frankenberg, C., & Kort, E. A. (2019). Interpreting contemporary trends in
491 atmospheric methane. *Proceedings of the National Academy of Sciences*, 116(8), 2805–
492 2813. <https://doi.org/10.1073/pnas.1814297116>

493 Unger, N. (2014). Human land-use-driven reduction of forest volatiles cools global climate.
494 *Nature Climate Change*, 4(10), 907–910. <https://doi.org/10.1038/nclimate2347>

495 Voulgarakis, A., Naik, V., Lamarque, J.-F., Shindell, D. T., Young, P. J., Prather, M. J., et al. (2013).
496 Analysis of present day and future OH and methane lifetime in the ACCMIP simulations.
497 *Atmospheric Chemistry and Physics*, 13(5), 2563–2587. [https://doi.org/10.5194/acp-13-](https://doi.org/10.5194/acp-13-2563-2013)
498 2563-2013

499 Wells, K. C., Millet, D. B., Payne, V. H., Deventer, M. J., Bates, K. H., de Gouw, J. A., et al. (2020).
500 Satellite isoprene retrievals constrain emissions and atmospheric oxidation. *Nature*,
501 585(7824), 225–233. <https://doi.org/10.1038/s41586-020-2664-3>

502 Whalley, L. K., Edwards, P. M., Furneaux, K. L., Goddard, A., Ingham, T., Evans, M. J., et al. (2011).
503 Quantifying the magnitude of a missing hydroxyl radical source in a tropical rainforest.
504 *Atmospheric Chemistry and Physics*, 11(14), 7223–7233. [https://doi.org/10.5194/acp-11-](https://doi.org/10.5194/acp-11-7223-2011)
505 7223-2011

506 Wiedinmyer, C., Tie, X., Guenther, A., Neilson, R., & Granier, C. (2006). Future Changes in
507 Biogenic Isoprene Emissions: How Might They Affect Regional and Global Atmospheric
508 Chemistry? *Earth Interactions*, *10*(3), 1–19. <https://doi.org/10.1175/EI174.1>

509 Wild, O., Voulgarakis, A., O'Connor, F., Lamarque, J.-F., Ryan, E. M., & Lee, L. (2020). Global
510 sensitivity analysis of chemistry–climate model budgets of tropospheric ozone and OH:
511 exploring model diversity. *Atmospheric Chemistry and Physics*, *20*(7), 4047–4058.
512 <https://doi.org/10.5194/acp-20-4047-2020>

513 Wolfe, G. M., Marvin, M. R., Roberts, S. J., Travis, K. R., & Liao, J. (2016). The Framework for 0-D
514 Atmospheric Modeling (FOAM) v3.1. *Geoscientific Model Development*, *9*(9), 3309–3319.
515 <https://doi.org/10.5194/gmd-9-3309-2016>

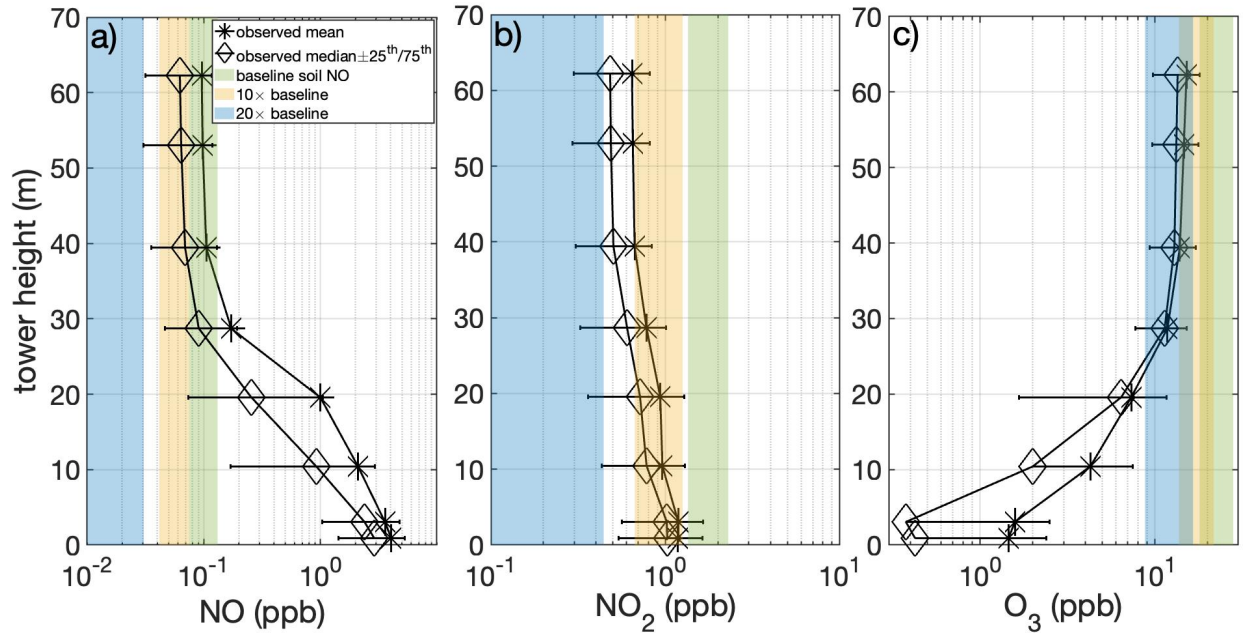
516 Wu, S., Mickley, L. J., Kaplan, J. O., & Jacob, D. J. (2012). Impacts of changes in land use and land
517 cover on atmospheric chemistry and air quality over the 21st century. *Atmospheric*
518 *Chemistry and Physics*, *12*(3), 1597–1609. <https://doi.org/10.5194/acp-12-1597-2012>

519 Yan, X., Ohara, T., & Akimoto, H. (2005). Statistical modeling of global soil NO_x emissions. *Global*
520 *Biogeochemical Cycles*, *19*(3). <https://doi.org/10.1029/2004GB002276>

521 Yienger, J. J., & Levy II, H. (1995). Empirical model of global soil-biogenic NO_x emissions. *Journal*
522 *of Geophysical Research: Atmospheres*, *100*(D6), 11447–11464.
523 <https://doi.org/10.1029/95JD00370>

524 Zhao, Y., Saunio, M., Bousquet, P., Lin, X., Berchet, A., Hegglin, M. I., et al. (2020). On the role of
525 trend and variability in the hydroxyl radical (OH) in the global methane budget. *Atmospheric*
526 *Chemistry and Physics*, *20*(21), 13011–13022. <https://doi.org/10.5194/acp-20-13011-2020>

527

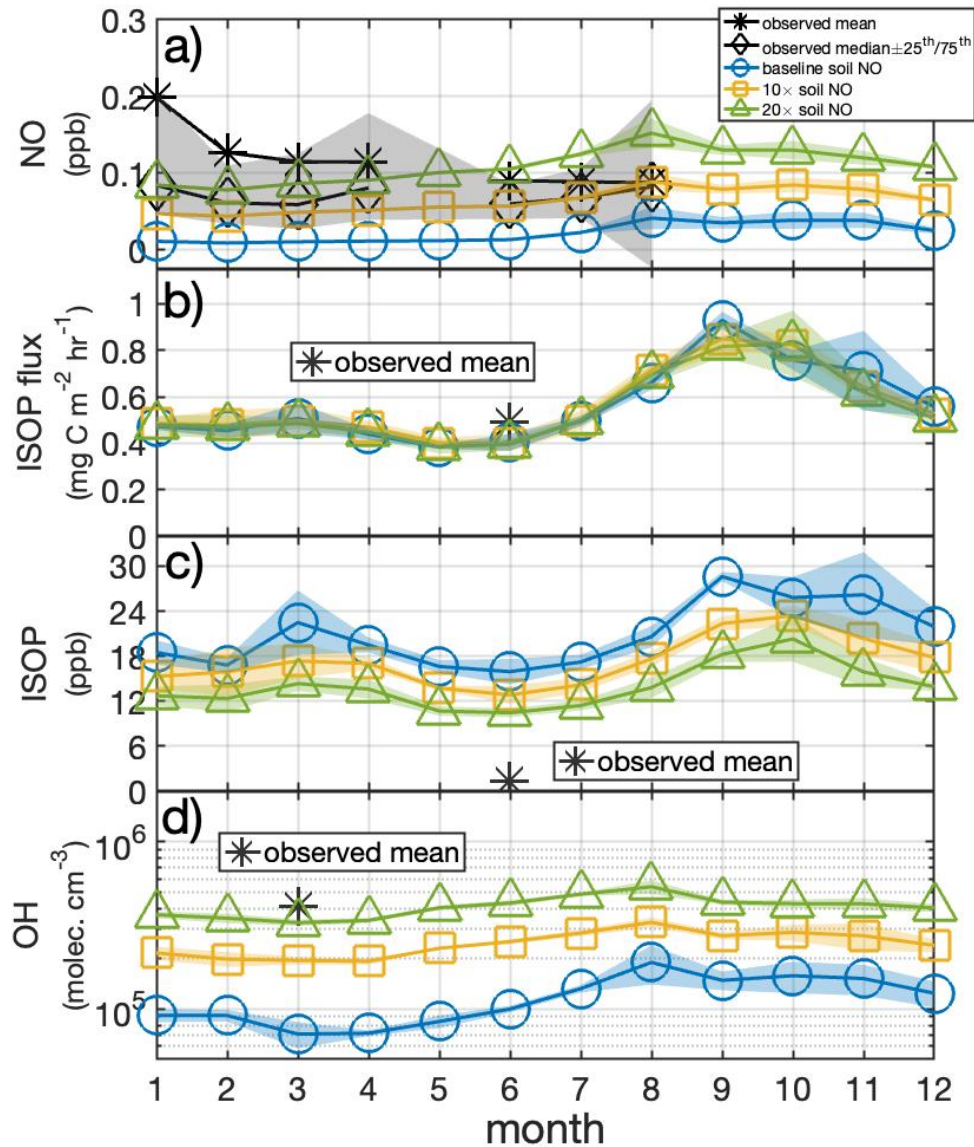


528

529

530 **Figure 1.** Mixing ratios of (a) NO, (b) NO₂, and (c) O₃ at the Tapajos National Forest as observed
 531 at eight heights on the tall tower from Jan to Aug of 2015, and as modeled for the lowest level
 532 of the atmosphere in CESM2-CAM-Chem under three soil NO emission rate scenarios. Model-
 533 observation comparison shows that soil NO emission rates in CESM2-CAM are biased low by at
 534 least an order of magnitude.

535



536

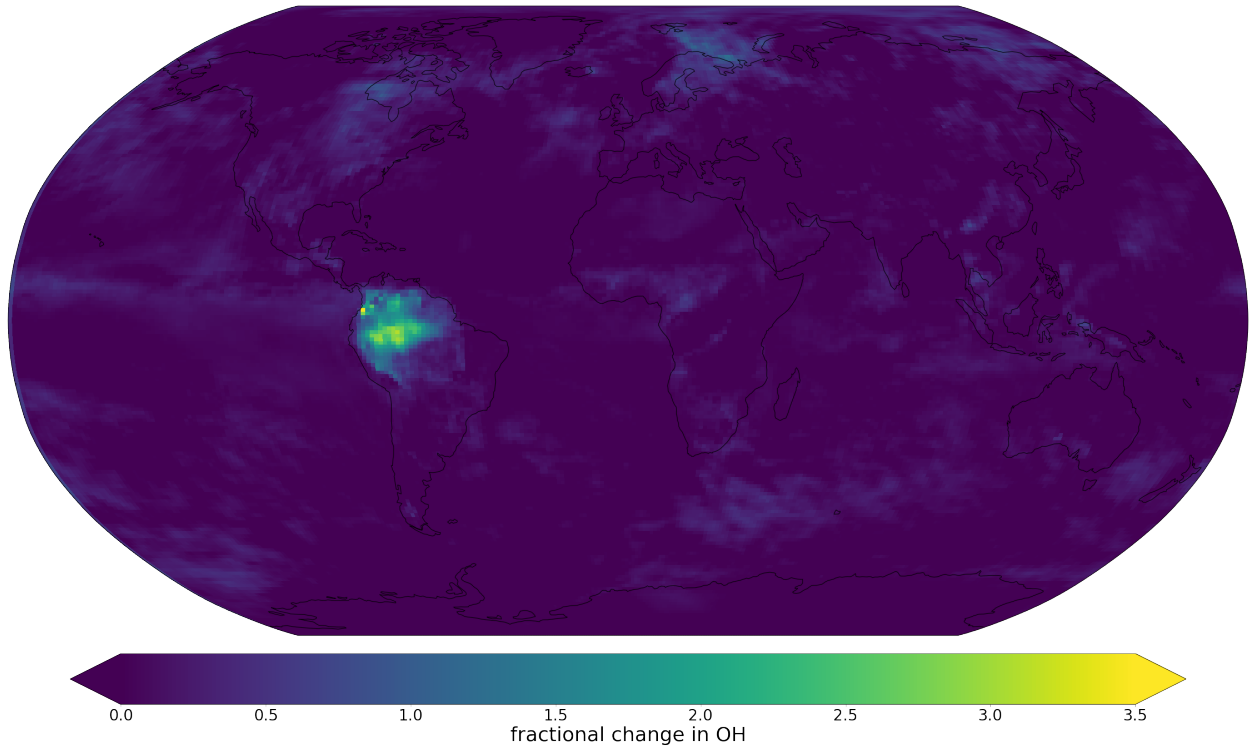
537

538 **Figure 2.** Monthly means of (a) NO mixing ratio, (b) isoprene flux, (c) isoprene mixing ratio, and
 539 (d) OH concentration in the lower-most level of the atmosphere above the Tapajos National
 540 Forest. Though there is general model-observation agreements in isoprene flux, NO mixing ratio
 541 and OH concentration by enhancing soil NO emission rate, there exists a large discrepancy in
 542 isoprene mixing ratio, indicating that accounting for the low-bias in soil NO emission rates does
 543 not fully resolve the high-bias in isoprene mixing ratio. Observations of isoprene flux and mixing
 544 ratios were conducted at the Tapajos National Forest in June of 2016 [Sarkar et al., 2020], while
 545 OH concentration was measured outside of Manaus, Brazil during GoAmazon in Feb-Mar of

546 2014 [Jeong et al., 2022]. Observed isoprene and OH values represent respective campaign
547 mean values.

548

549



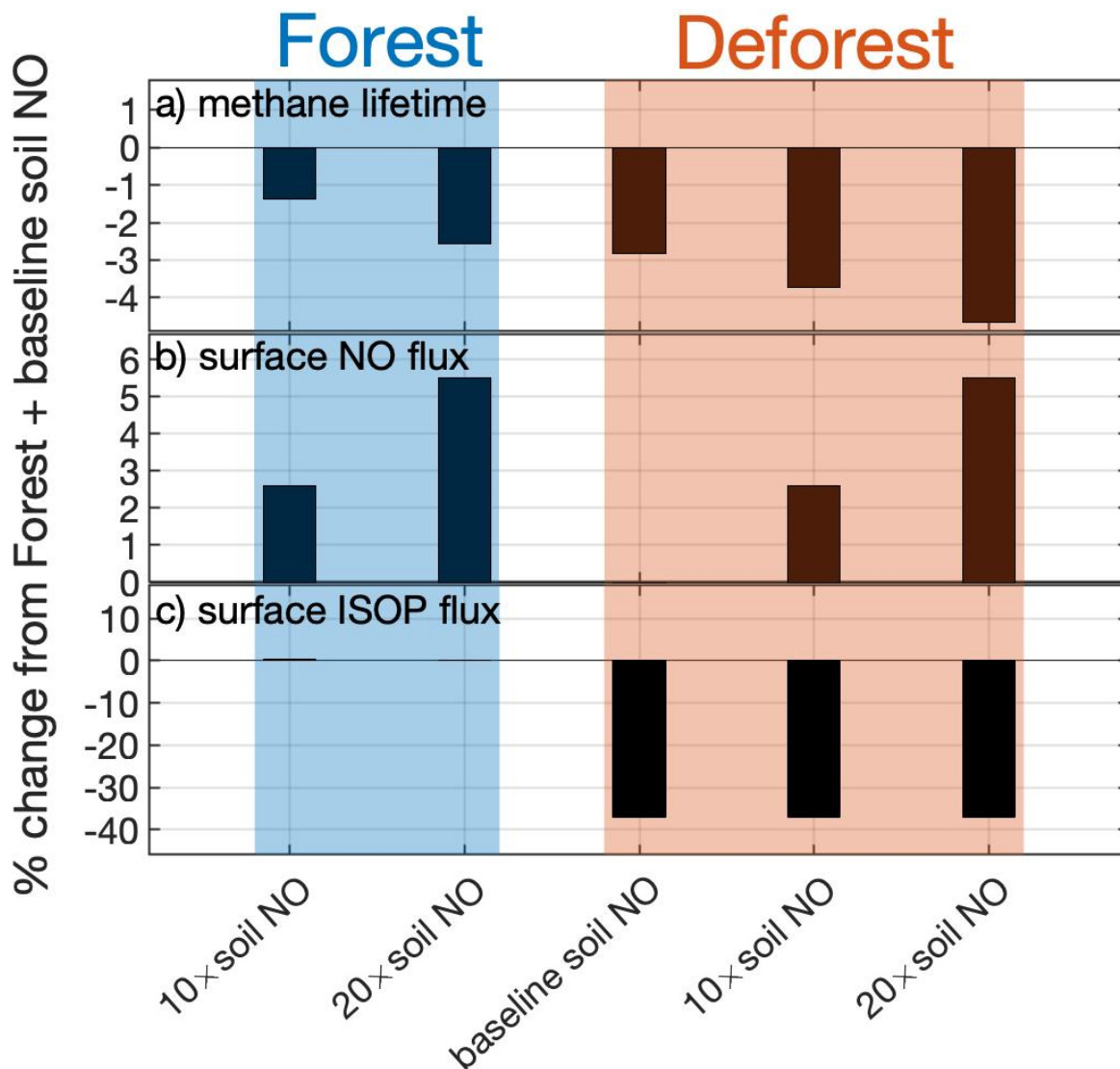
550

551

552 **Figure 3.** Fractional change in near-surface level (<800 hPa or <2 km) OH due to increasing soil
553 NO emissions from the Amazon by a factor of 20 relative to the baseline scenario in CESM2-
554 CAM-Chem for the month of September (wet season). Note the increase in OH due to
555 increasing soil NO emissions is evident in all seasons (**Figure 2d**).

556

557



558

559

560 **Figure 4.** Impact on global (a) methane lifetime (b) soil NO emission rates and (c) biogenic
 561 isoprene emission rates due to changes in soil NO emission rate of Amazonia and/or
 562 deforestation of Amazonia, relative to the forested Amazonia scenario with baseline NO
 563 emission rate of CESM2-CAM-Chem.

564

565